

# Optimization by Move–Class Deflation

Reimer Kühn<sup>1\*</sup>, Yu-Cheng Lin<sup>1</sup>, and Gerhard Pöppel<sup>2</sup>

<sup>1</sup> Institut für Theoretische Physik, Universität Heidelberg  
Philosophenweg 19, 69120 Heidelberg, Germany

<sup>2</sup> Uhlandstrasse 8, 93049 Regensburg, Germany

May 10, 1998

**Abstract:** A new approach to combinatorial optimization based on systematic move–class deflation is proposed. The algorithm combines heuristics of genetic algorithms and simulated annealing, and is mainly entropy–driven. It is tested on two problems known to be NP hard, namely the problem of finding ground states of the SK spin–glass and of the 3- $D \pm J$  spin–glass. The algorithm is sensitive to properties of phase spaces of complex systems other than those explored by simulated annealing, and it may therefore also be used as a diagnostic instrument. Moreover, dynamic freezing transitions, which are well known to hamper the performance of simulated annealing in the large system limit are not encountered by the present setup.

## 1 Introduction

Standard wisdom has it that strictly cost–decreasing algorithms are a bad choice for solving ‘hard’ optimization problems characterised by having huge numbers of locally optimal yet globally suboptimal solutions. The travelling salesman problem or the problem of finding ground–states of disordered frustrated systems such as the SK and the 3- $D \pm J$  spin–glasses are well known to belong to this category (for an overview, see [1]; another such problem, which has recently attracted some attention, is the binary–perceptron problem [2, 3, 4]). A common feature of these problems is that they have discrete phase spaces whose volume grows exponentially (or faster) with problem size, so that a complete enumeration of the universe of possible solutions as a means of finding the optimum is generally unfeasible. In terms of computational complexity [5], the three problems just mentioned are indeed known to be NP hard.

A number of algorithms have been invented to avoid getting trapped in local minima of cost- or energy functions — the most prominent and versatile among them being perhaps the simulated annealing algorithm [6, 7]. This approach introduces a mechanism of thermal activation accross barriers as implemented in the Metropolis algorithm [8] to escape from local minima of the cost function. The algorithm generates a Markov chain that approaches thermal equilibrium at a given temperature (if granted sufficient time to evolve), and as the temperature is gradually lowered to zero, thermal equilibrium singles out the ground state of the system, or one of the ground states in case of degeneracies. A problem with

---

\*Supported by a Heisenberg fellowship

this algorithm, though, is that equilibration times at low temperatures may be excessively large in large systems, and that the algorithm may *effectively* get trapped in suboptimal regions of configuration space because of time constraints. The design of efficient cooling schedules such as to make this at least an unlikely event has therefore always been of major concern of those working in the field. As a rule of thumb, it may be said that to devise an efficient cooling strategy always requires some tailoring depending on the system being investigated.

The so-called threshold-accepting algorithm [9] can be thought of as a variant of simulated annealing, the main difference being that unfavourable moves are accepted with uniform probability up to some threshold which is then gradually decreased to zero.

In population based algorithms of which the genetic ones [10] are perhaps the best known, a somewhat different approach is taken. Here a number of pairs within a ‘population’ of in general suboptimal solutions is selected and combined to form offspring which inherits usually equal parts of the solution of the optimization task from either parent. Specifically, if the solution to a complex optimization task is encoded in a bit-string of, say, length  $N$ , then the offspring will inherit  $\mathcal{O}(N/2)$  of the bits from one parent, and the remaining ones from the other, just as in sexual reproduction. The quality of the offspring is evaluated, and of the total new population now including the offspring, a certain fraction representing the fittest is retained to go for a new round of random pairing, offspring production and selection. Quite often, the genetic crossover process just described is combined with a certain rate of mutations, i.e. random changes of single bits in the copying process. Changes which involve mutation without crossover are also sometimes considered.

For things to come is useful to characterise the algorithms just described by their move class. In terms of a *distance* in phase space, as measured, e.g. by the Hamming distance of two bit-strings representing different solutions or – in spin-systems – by the number of overturned spins in a single move, the simulated annealing or threshold-accepting type algorithms are typically based on a set of *local* moves exploring distances  $d = \mathcal{O}(1)$  in phase space by a single move, whereas in genetic type algorithms the moves are non-local with  $d = \mathcal{O}(N/2)$ , sometimes mixed with  $d = \mathcal{O}(1)$  moves in cases using mutation without crossover.

In the present paper, we propose an alternative approach to complex optimization problems, based on a systematic tuning of move-classes from *macroscopic*, though usually  $\mathcal{O}(N)$ , to *microscopic* [11]. The strategy will be referred to as optimization by move-class deflation (OMCD) in what follows. It is perhaps best explained in terms of a specific example, viz. the problem of finding the ground state(s) of spin-glass Hamiltonians, such as that of the SK spin-glass [12] or that of the 3- $D \pm J$  spin-glass [13]. This will be done in Sect. 2, where we explain the heuristics, and verify it for the spin-glass problems, and analytically some aspects of it also on the toy problem of finding the ground-state of a Curie-Weiss ferromagnet. We shall see that OMCD makes *constructive use* of a feature which is generally considered as one of the most difficult problems to be overcome, namely of the usually very high dimensionality of the phase spaces in typical combinatorial optimization problems. Specifically, the feature we are able to *exploit* is the fact that local densities of state typically scale exponentially in system size.

In OMCD, the move-class deflation schedule plays a role analogous to the annealing schedule in the simulated annealing algorithm. Of particular interest here is the scaling of the initial size of the moves with the problem dimension  $N$ . This problem is dealt with in Sect. 3. In Sect. 4 we present results on ground-state energies of the spin-glass

problems introduced in Sect. 2, and on their scaling with system size. The MCD-algorithm is sensitive to properties of phase spaces of complex systems other than those ‘seen’ by simulated annealing, and it may thus be used as a new device for phase space diagnostics. This aspect is described in Sect. 5. Sect. 6 will conclude our paper with a summary and discussion.

## 2 The Heuristics of OMCD

Let us consider the problem of finding the ground state(s) of a spin-glass Hamiltonian such as

$$\mathcal{H}_N = - \sum_{(i,j)} J_{ij} S_i S_j , \quad (1)$$

where the  $S_i$ ,  $1 \leq i \leq N$ , denote Ising-spins with values in  $\{\pm 1\}$ . This Hamiltonian may represent an SK spin-glass [12] in which case the sum in (1) extends over all  $N(N-1)/2$  pairs of the system and the  $J_{ij}$  are assumed to be Gaussian random variables of mean  $\langle J_{ij} \rangle = J_0/N$  and variance  $\langle J_{ij}^2 \rangle - \langle J_{ij} \rangle^2 = 1/N$ . Alternatively, one may consider a model with short-range interactions such as the 3- $D$   $\pm J$  spin-glass [13], in which case the sum in (1) extends over all nearest neighbour pairs of a 3- $D$  simple cubic lattice, and the  $J_{ij}$  randomly take values in  $\{\pm 1\}$ .

Our strategy to find ground-states of (1) is as follows. We start from some randomly chosen initial spin configuration  $\mathbf{S}_0$ . Then we select a randomly chosen subset of the spins, containing (on average)  $d$  spins. Typically,  $1 \ll d \ll N$ . An attempt is made to flip these spins *simultaneously*. The attempt is accepted *only*, if it does not lead to an increase of  $\mathcal{H}_N$ , otherwise it is rejected. After this procedure has been repeated many times, the move-class is systematically ‘deflated’, e.g., by reducing the (average) size of the sets of spins suggested for a simultaneous flip by 1 ( $d \rightarrow d-1$ ), or by a certain factor ( $d \rightarrow \gamma d$ , with  $\gamma < 1$ ). And the procedure of proposing and accepting/rejecting simultaneous spin-flips depending on whether  $\mathcal{H}_N$  decreases or not continues with this smaller move class. Eventually the move-class is reduced to consist of single spin flips only, corresponding to zero-temperature Monte-Carlo dynamics. The scheme is characterised by the number of attempts at any given size of move-class and the way in which move-classes are deflated; this constitutes the move-class deflation schedule, which plays a role analogous to the cooling schedule in simulated annealing.

Why do we expect this scheme to give us good candidates for low-energy states and, given enough computer time, even ground-states? First, it is clear that by allowing macro-scoping moves, we can jump across energy barriers. If we allow occasional big moves to the very end, still allowing only moves that decrease (1), we are even *guaranteed* to find the bottom of the deepest energy valley eventually.

But why can we expect our method to be efficient? Well, this is a delicate question, and, as a matter of fact, we cannot expect this under all circumstances, e.g., when the energy landscape has a golf-course topology: almost everywhere flat with occasional small and narrow dips (optimization is generally difficult and slow in such situations). But for energy landscapes which are *normal* in the sense that, roughly speaking, deep valleys are also wide valleys, the following argument shows that our strategy for finding low-energy configurations should be an efficient one, even if the energy surfaces are rough in the sense of exhibiting complicated “valleys within valleys within valleys...” structures, which appears to be quite common for NP hard problems.

The first observation to make is that configuration spaces of the systems we are considering are usually characterised by having very high dimension. This circumstance, among others, is precisely what makes optimization difficult for these systems. For us *it is the starting point of our strategy*. One of the main consequences of high dimensionality is that almost all states of these systems have energies which are neither very high nor very low. The reason is that states of *typical* energy are near the “surface” of those regions in configuration space which have either rather high or rather low energy, and that virtually all volume of high dimensional objects is well known to be concentrated near their surface. In physics terms, states of typical energy have the largest (local) density of states (DOS). Since local densities of state typically scale exponentially in system size, states having an energy that differs significantly, i.e. on an extensive scale, from typical are exponentially (in system size  $N$ ) less probable than those having typical (hence average) energy. This observation is clearly confirmed in practice, and it might be called the *message of initialization*: picking an initial state  $\mathbf{S}_0$  of (1) at random, i.e. uncorrelated with the  $J_{ij}$ , we will *almost surely* find it to have zero energy (per spin) in the large system limit.

Running the OMCD algorithm, we start by making random macroscopic (or perhaps rather mesoscopic) moves which are accepted if they do not increase the energy. Were do we get? At states which have both, a high probability — otherwise they would not have been selected at random — and a lower energy, because only moves which lower (or at least do not increase) the energy are accepted. Such states may be expected to be near the surface (“half up”) of both wide and deep valleys. Eventually, the macroscopic moves suggested will no longer be accepted, because being macroscopic, they would lead us outside or higher up the wide and deep valley we have already found. The probability of selecting some state which may be deep inside some other (narrower and in the end suboptimal) valley — that is, lower in energy than half up the deep and wide valley we have already found — can be considered negligibly small in the large system limit because of entropy (density of state) considerations as discussed above. Next, the move-class is reduced, so that states *within* the valley we have already selected can be reached and are accepted if they lower (or do not increase) the energy. By the same argument as before, we may expect to arrive at states near the surface of the deepest and widest valley structures *inside* the valley we have already selected. Moreover, since the move-class contains only smaller moves, a larger — and by our reasoning irrelevant — part of the phase space is already effectively shielded from our search. Having arrived at this finer level, we can repeat our argument as before, with a move class that is reduced once more. By systematically reducing the move class, we thus explore the energy landscape down to the deepest and finest structures, shielding off larger and larger parts of phase space from our search as we go along.

Note that the “effective” dimension of the accessible configuration space goes down as the search proceeds, and entropy/DOS arguments might become less forceful as we are homing in on low energy configurations. One might therefore consider the possibility of switching the strategy towards an exhaustive search of the configuration space (within a small Hamming distance of some state already reached) in the final stage of an optimization run.

The above considerations can be verified quantitatively for the toy-problem of finding the ground state of a Curie-Weiss ferromagnet

$$\mathcal{H}_N = -\frac{N}{2}m^2, \quad (2)$$

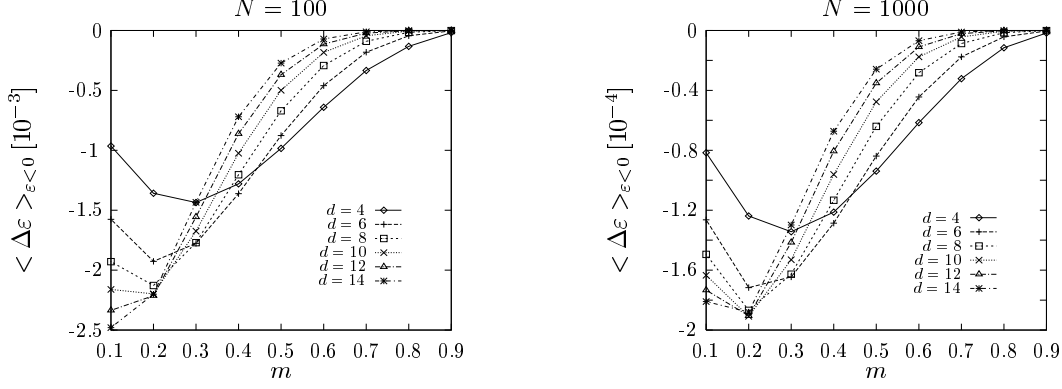


Figure 1: Average energy change  $\langle \Delta \varepsilon \rangle$  through accepted moves in OMCD as a function of the magnetization  $m$  for the Curie Weiss model, for various sizes  $d$  of the move class. Left: system size  $N = 100$ . Right: system size  $N = 1000$ . Evaluation according to Eqs (2) – (6).

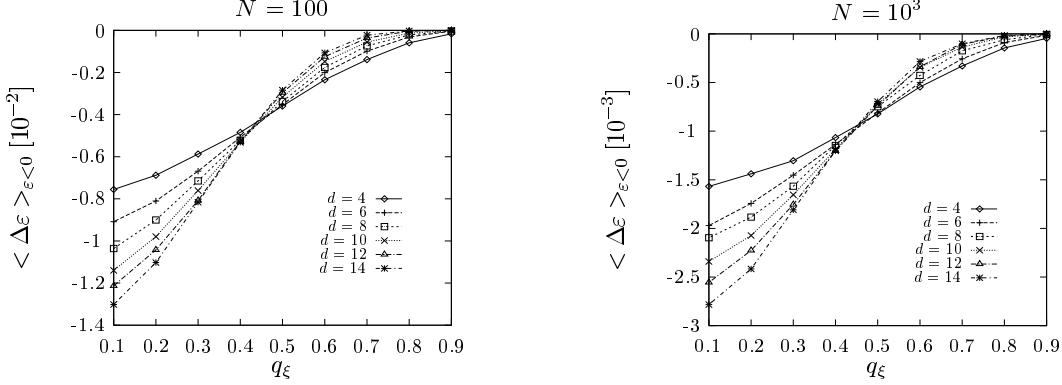


Figure 2: Simulation results for average energy change  $\langle \Delta \varepsilon \rangle$  through accepted moves in OMCD as a function of the overlap  $q_\xi$  with a ground-state configuration for the SK model (left) and the  $\pm J$  model (right), for various sizes  $d$  of the move class. The system sizes are  $N = 100$  and  $N = 1000$ , respectively.

with  $m$  denoting the magnetisation (per spin) of the system. For a move class of size  $d$ , the probability to select  $r$  out of  $d$  spins with  $S_i = -1$  is given by

$$\mathcal{P}_r = \binom{d}{r} p^r (1-p)^{d-r}, \quad \text{with } p = \frac{1-m}{2}. \quad (3)$$

Flipping  $r$  negative spins changes the magnetization (per spin) by

$$\Delta m = \frac{2}{N} (2r - d) \quad (4)$$

and thus the energy (per spin) by

$$\Delta \varepsilon = -\frac{1}{2} (\Delta m)^2 - m \Delta m. \quad (5)$$

We can express  $\Delta m$  (hence  $r$ ) in terms of  $m$  and  $\Delta \varepsilon$

$$\Delta m = -m + \sqrt{m^2 - 2\Delta \varepsilon} \quad (6)$$

which allows us, using (3), to compute the average decrease in energy  $\langle \Delta \varepsilon \rangle$  from moves of size  $d$  within the MCD algorithm as a function of the magnetization  $m$ . (To evaluate the average, we use the Stirling approximation  $k! \simeq \sqrt{2\pi k} k^k \exp\{-k + \frac{1}{12k}\}$  to compute factorials of large numbers.) The result is shown in Fig. 1, and it demonstrates that, depending on the distance to the minimum of the energy it appears to be advantageous to change from larger to smaller moves as the fully magnetized configuration (i.e. the state of minimal energy) is approached. In Fig. 2 we show for comparison that qualitatively similar results are obtained for the SK spin-glass and for the 3- $D$   $\pm J$  model, if the magnetization is replaced by the overlap  $q_\xi = N^{-1} \sum_i \xi_i S_i$  between the system state  $\mathbf{S}$  and a ground-state configuration  $\{\xi_i\}$ .

### 3 Scaling Properties

In OMCD, the move-class deflation schedule plays a role analogous to the annealing schedule in simulated annealing. Of primary interest here is the size  $d = d_0$  of the initial moves required to find good ground states in the end. Clearly the initial size of the move-class should be chosen such as to allow to jump over (or perhaps more appropriately tunnel through) the widest energy barriers which might typically separate an initially chosen random configuration from a good ground-state configuration.

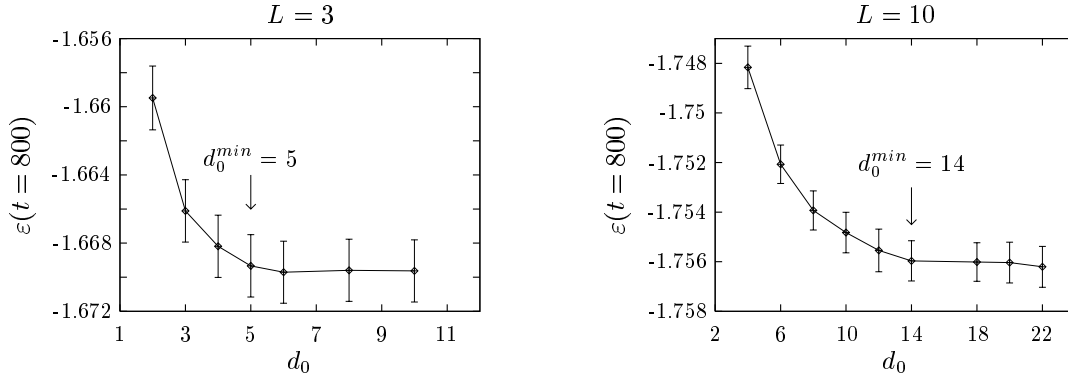


Figure 3: Best energies, obtained with  $t = 800$  MCS at each  $d$ , for the  $\pm J$  model of size  $N = L^3$  as a function of the initial size  $d_0$  of the move-class. Left:  $L = 3$ , right:  $L = 10$ . Results are averages over  $M = 4000$  samples for  $L = 3$ , and over  $M = 350$  for  $L = 10$ , and are displayed along with statistical errors  $\sigma = \sqrt{\text{var}(\varepsilon)/M}$ .

In spin-glasses, the barrier-heights are well known to scale with system size. For instance, in case of the SK model numerical [14] and analytical [15, 16] investigations indicate a divergence of the barrier heights  $\Delta E$  with system size  $N$  according to

$$\Delta E \sim N^\lambda, \quad \text{with} \quad \lambda \simeq \frac{1}{3}. \quad (7)$$

We are currently not aware of quantitative studies of this issue for the  $\pm J$  model, although some divergence with  $N$  is to be expected for this case as well. If the energy landscapes of the SK and  $\pm J$  models are ‘normal’ in the sense described above, we have to anticipate a divergence of the barrier-widths with system size as well. Within OMCD this should manifest itself through the fact that we need a *minimal* initial size  $d_0$  of the move-class, in order to arrive at good low-energy configurations as the algorithm proceeds.

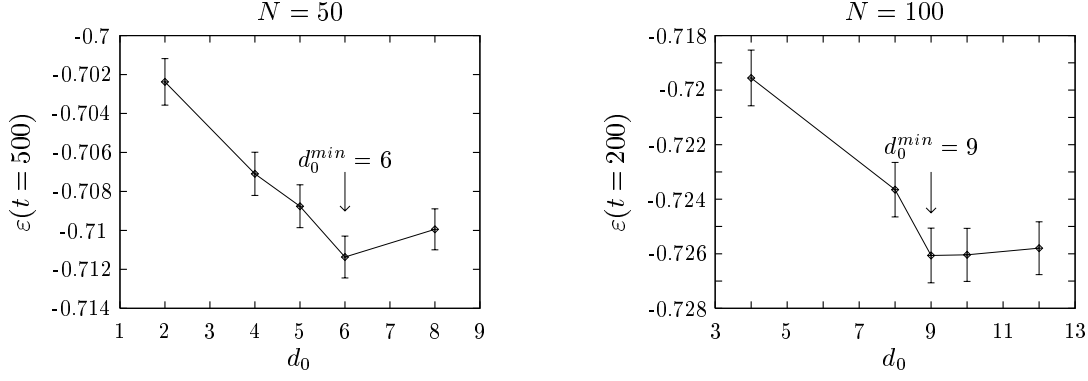


Figure 4: Best energies  $\varepsilon(t)$ , obtained with  $t$  MCS at each  $d$ , for the SK model of sizes  $N = 50$  (left) and  $N = 100$  (right) as a function of the initial size  $d_0$  of the move-class. Results are displayed along with statistical errors. Averages are performed over 2000 and 500 samples respectively.

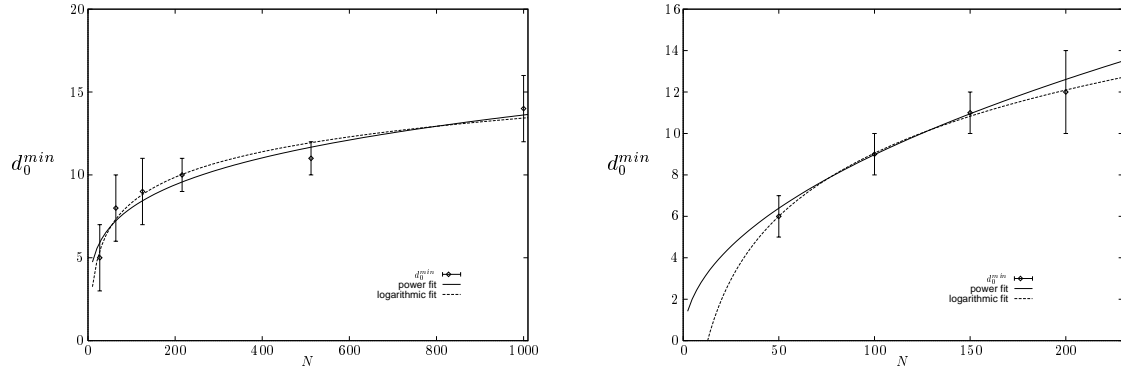


Figure 5:  $d_0^{min}$  as a function of system size  $N$  for the  $\pm J$  model (left) and the SK model (right), with power-law and logarithmic fits.

Figs. 3 and 4 show results for final energies obtained by OMCD as a function of the initial size  $d_0$  of the move class for  $\pm J$  and SK models of different sizes. From such simulations, we can extract  $d_0^{min}$  as a function of system size  $N$ , and extract its scaling with  $N$ . For both cases we have attempted two types of fit, using the `mrqmin` routine from Press et al. [17] (see Fig. 5), namely

$$d_0^{min} = a_1 N^{b_1} \quad (8)$$

$$d_0^{min} = a_2 + b_2 \ln N \quad (9)$$

for large  $N$ .

	$\pm J$ -model	SK-model
$a_1$	$2.79 \pm 0.61$	$0.94 \pm 0.55$
$b_1$	$0.23 \pm 0.04$	$0.49 \pm 0.12$
$a_2$	$-1.90 \pm 1.77$	$-11.19 \pm 4.55$
$b_2$	$5.11 \pm 0.77$	$10.12 \pm 2.21$

Table 1: Values for the fit parameters appearing in Eqs. (8) and (9).

The results are collected in Table 1 and Fig. 5. Somewhat to our surprise, we find that

the logarithmic fits are consistently (though only slightly) better than the power-law fits. We obtained  $Q_{\pm J} = 0.76$  and  $Q_{SK} = 0.98$  for the logarithmic fits and  $Q_{\pm J} = 0.65$  and  $Q_{SK} = 0.86$  for the power-law fit as measured by the `mrqmin` routine [17]. It would – at least for the SK model – be difficult to reconcile this with a ‘normality’ assumption about the energy landscape of this model, if we accept the fact that we have to tackle energy barriers scaling with system size  $N$  as indicated in (7). However, the following observation might be advanced in favour for the correctness of the logarithmic scaling anyway. It is not excluded, in particular for the large system sizes, that OMCD does not have to surmount the largest (hence widest) energy barriers at all, because due to the exponential scaling (in  $N$ ) of the local DOS, the random initialization would with sufficiently high probability already select a state near the surface of the deepest and widest valley, so that the largest and widest energy barriers need in fact not be passed through at all. In this context one might recall that Kinzelbach and Horner [15, 16] observed that the spectrum of relaxation times for the finite SK model contains one with the weakest system-size dependence, scaling as  $\tau \sim N^\nu$  with system size  $N$ . Assuming such a scaling to be due to an Arrhenius type mechanism with an activation energy barrier  $B_N$ , that is  $\tau \sim \exp\{B_N/k_B T\}$ , one would have to conclude that this type of barrier exhibits a logarithmic scaling with system size  $B_N \sim \ln N$ , and it is possible that we have to tackle only these very weakly diverging barriers in OMCD, as the system size becomes large. This point clearly deserves a deeper and more extensive study.

## 4 Ground-State Energies of Spin-Glasses

We have used OMCD to determine ground state energies of the 3- $D$   $\pm J$  spin-glass and of the SK model. Following [1], we have recorded the lowest energies found by the MCD algorithm as a function of the time  $t$ , measured by the number of attempted moves per spin (MCS) spent at each move-class size  $d$ . In analogy to the findings of these authors, we observe a logarithmic dependence of the form

$$\varepsilon(t) = \varepsilon_{min} + c_1/\ln t ; \quad (10)$$

see Figs. 6 and 7. This is due to the fact that the problem of finding true ground-states for these systems is believed to be NP-hard.

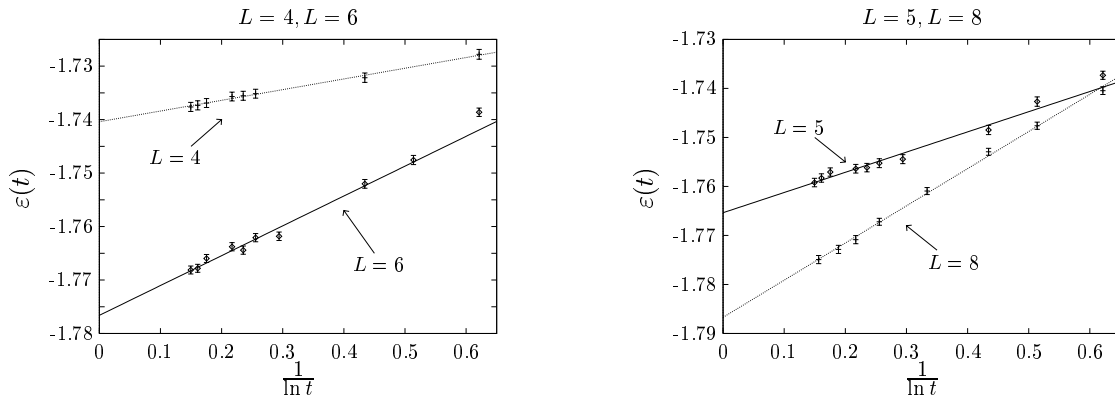


Figure 6: Best energies obtained for  $\pm J$  models of various sizes as a function of the time  $t$  measured in MCS spent at each size  $d$  of the move-class, exhibiting the logarithmic scaling of Eq. (10).



3D $\pm J$ -model								
$L = 3$ ( $I_N = 3, d_0 = 6$ )					$L = 4$ ( $I_N = 4, d_0 = 8$ )			
$t$	$M_N$	$\varepsilon_N(t)$	$\sigma(\varepsilon)$	$\tau(s)$	$M_N$	$\varepsilon_N(t)$	$\sigma(\varepsilon)$	$\tau(s)$
5	18000	-1.667647	0.000887	0.03	5000	-1.727787	0.000921	0.09
10	18000	-1.670881	0.000863	0.06	5000	-1.732162	0.000880	0.18
50	18000	-1.673235	0.000866	0.26	5000	-1.735146	0.000832	0.90
70	—	—	—	—	5000	-1.735542	0.000841	1.25
100	—	—	—	—	5000	-1.735687	0.000828	1.78
300	18000	-1.673009	0.000826	1.65	5000	-1.736896	0.000839	5.32
500	—	—	—	—	5000	-1.737333	0.000857	8.87
800	—	—	—	—	5000	-1.737625	0.000849	14.18
1000	18000	-1.672839	0.000865	5.50	—	—	—	—
$L = 5$ ( $I_N = 4, d_0 = 10$ )					$L = 6$ ( $I_N = 5, d_0 = 12$ )			
$t$	$M_N$	$\varepsilon_N(t)$	$\sigma(\varepsilon)$	$\tau(s)$	$M_N$	$\varepsilon_N(t)$	$\sigma(\varepsilon)$	$\tau(s)$
5	3000	-1.737312	0.000836	0.39	2000	-1.738620	0.000781	0.86
7	2000	-1.742681	0.000957	0.50	1500	-1.747556	0.000855	1.25
10	2000	-1.748480	0.000945	0.71	1500	-1.752012	0.000819	1.71
30	2000	-1.754432	0.000923	2.13	1500	-1.761815	0.000793	5.11
50	2000	-1.755248	0.000907	3.60	1500	-1.762077	0.000769	8.49
70	2000	-1.756168	0.000864	5.04	1500	-1.764412	0.000767	11.90
100	2000	-1.756384	0.000876	7.12	1500	-1.763781	0.000768	17.02
300	2000	-1.757060	0.000847	21.36	1500	-1.765975	0.000749	51.00
500	2000	-1.758281	0.000854	35.58	1500	-1.767815	0.000741	85.00
800	2000	-1.759207	0.000862	57.20	1500	-1.768124	0.000743	135.93
$L = 8$ ( $I_N = 15, d_0 = 12$ )								
$t$	$M_N$	$\varepsilon_N(t)$	$\sigma(\varepsilon)$	$\tau(s)$				
5	700	-1.740453	0.000784	1.73				
7	700	-1.747612	0.000735	2.41				
10	700	-1.752922	0.000710	3.45				
20	700	-1.760937	0.000716	6.92				
50	700	-1.767210	0.000702	17.48				
100	500	-1.770859	0.000835	34.45				
200	500	-1.772844	0.000835	68.75				
600	500	-1.774922	0.000834	207.08				

Table 2: Lowest energies of  $\pm J$ -models found, as a function of  $t$  measured in units of MCS/spin, and system size  $N = L^3$ . We also record the statistical error and the average time needed for a *single* OMCD run on a 100 MHz 486DX-PC.  $M_N$  is the number of bond configurations used for averaging,  $I_N$  is the number of runs at each bond configuration, from which the minimum was selected.

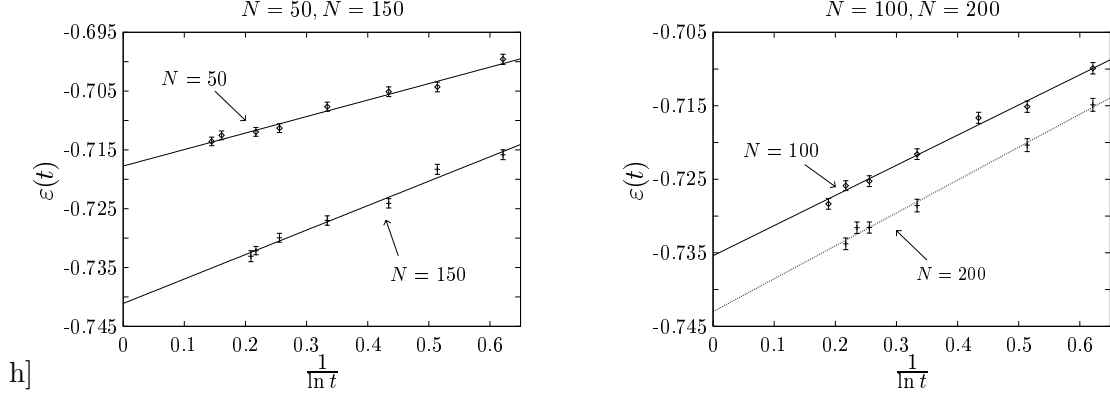


Figure 7: Best energies obtained for SK models of various sizes as a function of the time  $t$  measured in MCS spent at each size  $d$  of the move-class.

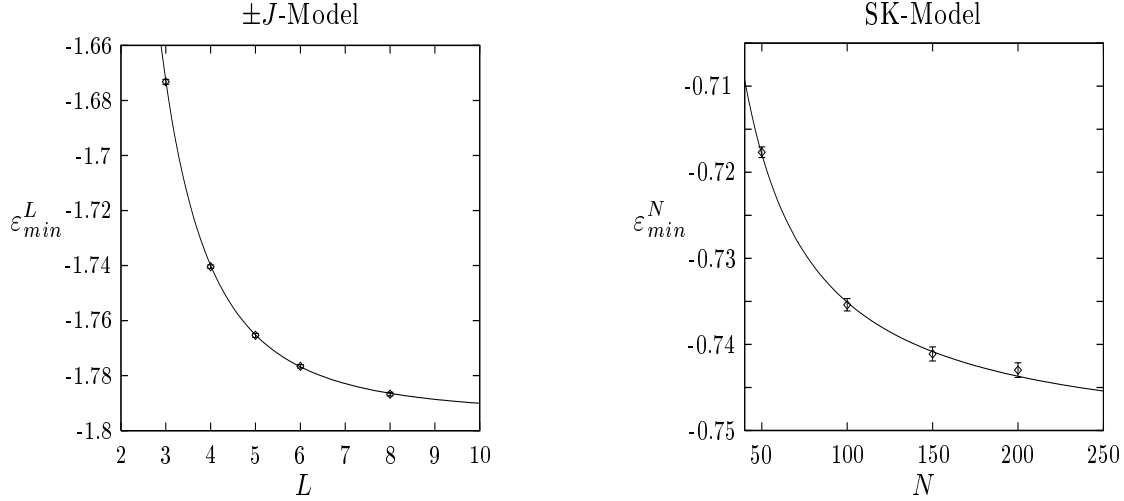


Figure 8: Finite size scaling of the ground state energies of the  $\pm J$  model and the SK model, respectively.

For the  $\pm J$  model, we have investigated systems of size  $L^3$ , with  $L = 3, 4, 5, 6$ , and  $8$ . For the SK model we have looked at system sizes  $N = 50, 100, 150$ , and  $200$ . The initial size  $d_0$  of the move-class was chosen according to the results of the scaling-analysis of the previous section. In the case of the  $\pm J$  model, the  $d$  spins to be flipped in a move-class of size  $d$  were selected by a random walk which visited  $d$  sites, with starting point selected serially (or at random). In the case of the SK model, the  $d$  spins were simply selected at random.

For each system (each bond configuration),  $I_N$  optimization runs were performed, and only the absolute energy minimum among these runs was recorded. Results were averaged over  $M_N$  random bond configurations, with  $M_N$  ranging from 18000 for the small systems to 500 for the large systems (and large  $t$ ) in the case of the  $\pm J$  model, and similarly from 2000 to 300 in the case of the SK model. Our results are collected in Tables 2 and 3 (which also records the average time needed for a *single* OMCD run on a 100 MHz 486DX-PC).

Tables 4 and 5 contain  $t \rightarrow \infty$ -extrapolations of the lowest energies found according to

SK-model								
$N = 50$ ( $I_N = 5, d_0 = 6$ )					$N = 100$ ( $I_N = 8, d_0 = 9$ )			
$t$	$M_N$	$\varepsilon_N(t)$	$\sigma(\varepsilon)$	$\tau(s)$	$M_N$	$\varepsilon_N(t)$	$\sigma(\varepsilon)$	$\tau(s)$
5	2000	-0.699584	0.000857	0.22	1000	-0.709894	0.000775	1.77
7	2000	-0.704299	0.000857	0.30	1000	-0.715125	0.000765	2.51
10	2000	-0.705108	0.000824	0.43	1000	-0.716640	0.000756	3.53
20	2000	-0.707653	0.000783	0.87	1000	-0.721576	0.000728	7.02
50	2000	-0.711303	0.000748	2.15	1000	-0.725257	0.000740	17.77
100	2000	-0.711930	0.000750	4.26	1000	-0.725867	0.000670	35.49
200	—	—	—	—	800	-0.728344	0.000730	70.89
500	2000	-0.712526	0.000745	21.00	—	—	—	—
1000	2000	-0.713555	0.000733	42.40	—	—	—	—
$N = 150$ ( $I_N = 15, d_0 = 11$ )					$N = 200$ ( $I_N = 20, d_0 = 12$ )			
$t$	$M_N$	$\varepsilon_N(t)$	$\sigma(\varepsilon)$	$\tau(s)$	$M_N$	$\varepsilon_N(t)$	$\sigma(\varepsilon)$	$\tau(s)$
5	500	-0.715820	0.000832	5.98	300	-0.714866	0.000872	12.35
7	500	-0.718296	0.000849	8.23	300	-0.720348	0.000885	17.30
10	500	-0.724086	0.000794	11.72	—	—	—	—
20	500	-0.727007	0.000802	23.19	300	-0.728572	0.000866	48.87
50	500	-0.729938	0.000758	58.12	300	-0.731563	0.000754	121.50
70	—	—	—	—	300	-0.731578	0.000784	171.66
100	500	-0.732130	0.000713	115.92	300	-0.733769	0.000795	243.89
120	300	-0.733078	0.000928	139.12	—	—	—	—

Table 3: Lowest energies of SK-models found, as a function of  $t$  measured in units of MCS/spin, and system size  $N$ . Symbols are defined as in Table 2.

Eq. (10), and compare with results of Refs. [1], [18] – [21]. Note that  $t \rightarrow \infty$  extrapolations were not performed in [18] – [21]. The results of Berg et al. [18] were obtained using multicanonical sampling, those of [19, 20, 21] by combining the genetic algorithm with some other strategy, whereas [1] used simulated annealing.

The finite-size signature of the true average ground state energies was extracted to follow the scaling

$$\varepsilon_{min}^L = \varepsilon_{min}^\infty + a_1 L^{-a_2} \quad (11)$$

with

$$\varepsilon_{min}^\infty = -1.7942(10) \quad , \quad a_1 = 2.63(19) \quad , \quad a_2 = 2.80(7) \quad (12)$$

for the 3- $D \pm J$  model on cubes of side-length  $L$ , and the scaling

$$\varepsilon_{min}^N = \varepsilon_{min}^\infty + \frac{b}{N} \quad (13)$$

with

$$\varepsilon_{min}^\infty = -0.7523(8) \quad , \quad b = 1.72(6) \quad (14)$$

for the SK model (the deviation of 1.5% from the analytic result [22] might be due to the fact that the groundstate energy of the largest system used in our fit is perhaps somewhat poor). Results along with the above fits are shown in Fig. 8.

So far we have paid little attention to details of the deflation schedule apart from its starting with a sufficiently large move-class, i.e. to the *optimization of the optimization*

3D $\pm J$ -model						
	$\varepsilon_{min}^L$					
$L$	this work	Ref. [1]	Ref. [18]	Ref. [19]	Ref. [20]	Ref. [21]
3	-1.6732(9)	—	—	-1.68138	-1.67171	-1.6731
4	-1.7404(6)	-1.791	-1.7378	-1.73973	-1.73749	-1.7370
5	-1.7654(7)	—	—	-1.76101	-1.76090	-1.7603
6	-1.7766(6)	—	-1.7674	-1.77059	-1.77130	-1.7723
7	—	—	—	-1.77842	-1.77706	—
8	-1.7867(7)	—	-1.7799	-1.77901	-1.77991	-1.7802
10	—	—	—	—	-1.78339	-1.7840
12	—	—	-1.7936	—	-1.78407	-1.7851
14	—	—	—	—	-1.78653	-1.7865

Table 4: Ground state energies for the 3- $D \pm J$  model of various sizes.

SK-model		
	$\varepsilon_{min}^N$	
$N$	this work	Ref. [1]
50	-0.7177(6)	-0.7174
100	-0.7354(7)	-0.7354
150	-0.7411(8)	—
200	-0.7430(9)	-0.7472
400	—	-0.7534
800	—	-0.7591
1300	—	-0.7620

Table 5: Ground state energies for SK models of various sizes.

*algorithm itself.* The above results were obtained using a linear decrease  $d \rightarrow d - 1$  of the size of the move-class, starting from  $d_0$  as determined in the previous section. Other deflation schedules may clearly be considered. Here we briefly mention the ‘exponential’ schedule

$$d \rightarrow \lceil \gamma d \rceil, \quad \text{with } \gamma < 1, \quad (15)$$

where  $\lceil x \rceil$  denote the largest integer less than or equal to  $x$ . This schedule is approximately exponential for large  $d$ , and it crosses over to linear, as soon as  $\gamma d > d - 1$ . We have compared the results of such a schedule with  $\gamma = 0.8$  on the  $\pm J$  model of size  $N = 5^3$  and on the SK model with  $N = 100$  for various  $t$ . The change in the estimate of the lowest energy is in the 0.2% range, while the computational cost was measured to decrease by roughly 40% in the case of the  $\pm J$  model, and by roughly 30% for the SK model! This little study shows that there may still be room for considerable improvements of the algorithm itself, improvements which might clearly benefit from tailoring in problem specific ways.

## 5 Phase-Space Diagnostics

As we have mentioned in our introduction, and also when describing the heuristics of OMCD, the MCD algorithm is sensitive to properties of phase spaces of complex systems other than those seen by simulated annealing. For instance, deep down in a narrow valley

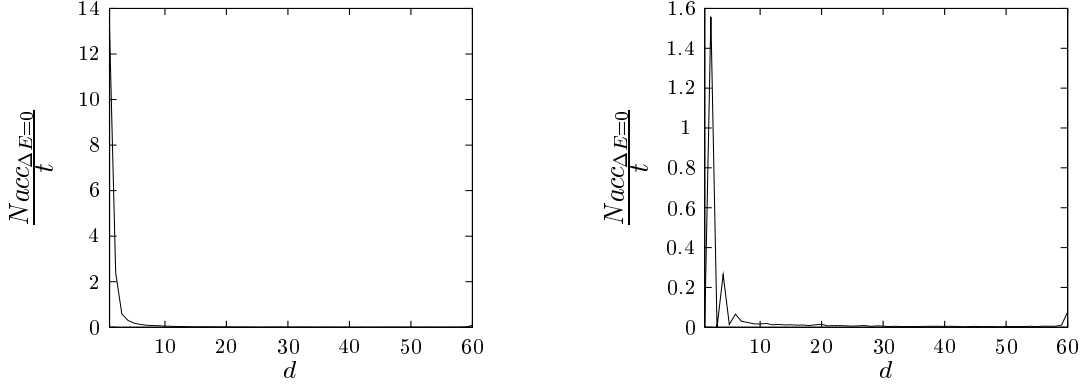


Figure 9: Number of moves accepted per MCS with  $\Delta E = 0$  in the  $\pm J$  model (left) and the ferromagnet (right), as a function of the size  $d$  of the move-class. The system size is  $N = 216$ .

large moves will not be accepted because they could only lead us uphill (or perhaps outside the valley we are currently in). This observation might in the future be used to develop strategies for self-optimization of the move-class deflation schedule as it proceeds with any given optimization task.

Here we illustrate this feature by monitoring — for the  $\pm J$  and the SK model (and also for a simple 3- $D$  ferromagnet) — the number of accepted moves per MCS which decrease the energy, as a function of the size  $d$  of the move-class, which is deflated linearly. For the  $\pm J$  model and the ferromagnet, we have separately monitored the moves which are accepted but lead to a degenerate state. Such moves with  $\Delta E = 0$  in the  $\pm J$  model and the ferromagnet occur predominantly at very small  $d$ , as seen in Fig 9.

Fig. 10 shows clear differences between the SK model on the one hand side and the  $\pm J$  model and the ferromagnet on the other side. Apart from the ‘transient’ behaviour near the initially chosen largest move class size, there is a clear trend for the SK model towards acceptance of predominantly small moves, whereas this feature is much less pronounced in the other two models. On the other hand, there seems to be some systematic depression of the acceptance rate in the  $\pm J$  model near  $d = 47$  and  $d = 40$ , which survives the averaging over different bond-configurations implied in the representation of Fig. 10.

Whether the difference between the SK model on the one hand side and the  $\pm J$  model and the ferromagnet on the other side is due to the discreteness of the energy spectrum in the latter two models which is not shared by the SK model, or due to the fact that the phase spaces of these models are in different complexity classes, we can at present not tell: It is well known that the SK model has a non-trivial distribution of overlaps between its various ground states. For the  $\pm J$  model this issue is currently still under debate, while in the ferromagnet, the overlap distribution is known to be trivial (i.e., to consist of two delta functions at  $\pm 1$ ).

## 6 Summary and Discussion

In summary, we have proposed an alternative approach to complex combinatorial optimization problems named OMCD, based on a systematic deflation of move-classes from mesoscopic to microscopic. The algorithm combines heuristics of genetic algorithms and

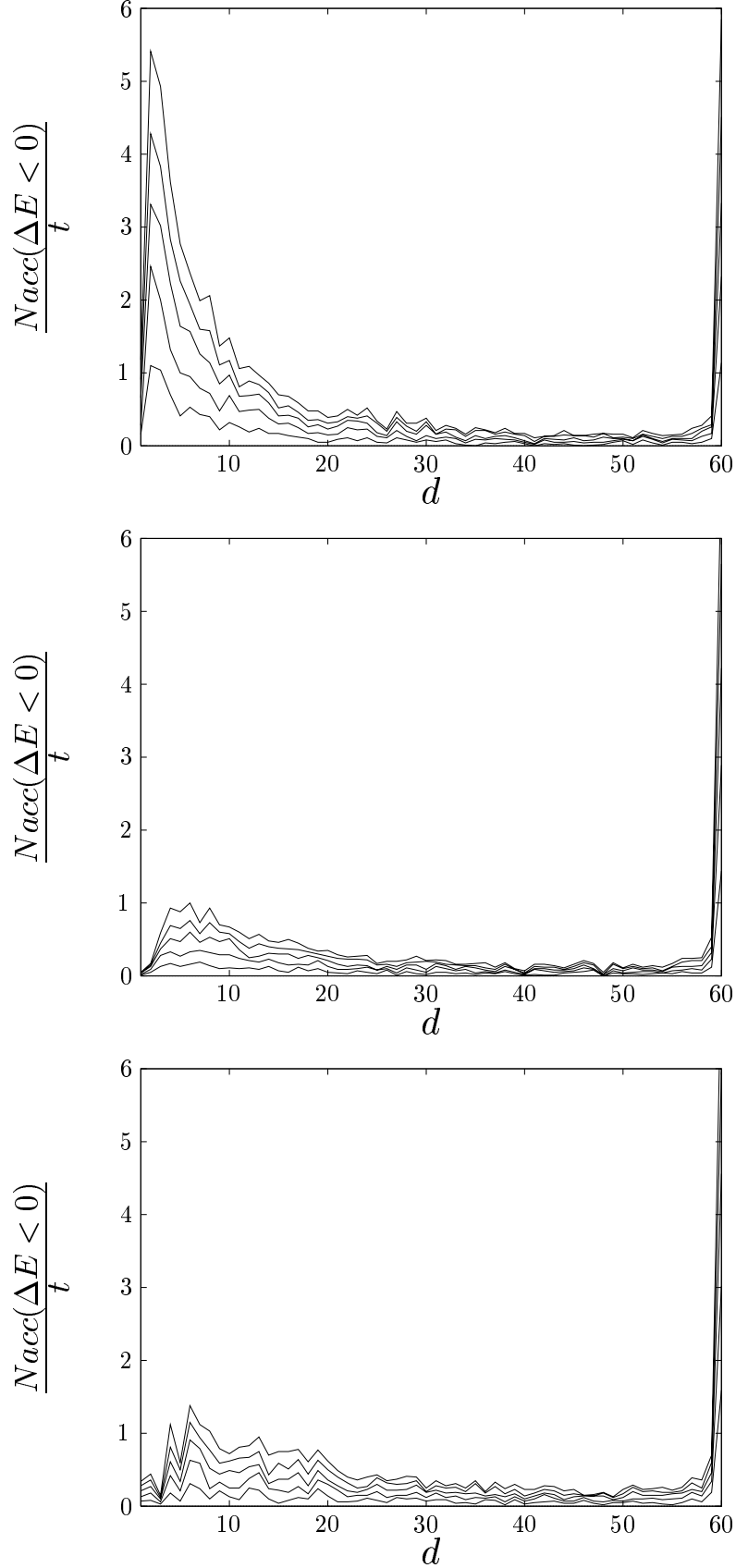


Figure 10: Number of moves accepted per MCS with  $\Delta E < 0$  in the SK model, the  $\pm J$  model, and the ferromagnet (from top to bottom), as a function of the size  $d$  of the move-class, accumulated over 10, 20, 30, 40, and 50 samples. The system size is  $N = 216$  in all cases, and  $t = 100$ .

simulated annealing. We expect it to be efficient for problems with energy surfaces which are normal in the sense that deep valleys are also wide valleys (and correspondingly high barriers are also wide barriers). We have argued that it makes *constructive* use of the high dimensionality of phase spaces typically encountered in large combinatorial optimization tasks, specifically of the exponential scaling of (local) densities of state with system size  $N$ . That is, the algorithm *exploits* a feature which is generally believed to constitute a major difficulty to be tackled in combinatorial optimization. It is perhaps worth mentioning that local densities of state do play a role also in the dynamics of other combinatorial optimization algorithms, if perhaps less explicitly (or less consciously) so.

We have verified our heuristics analytically on the toy-problem of finding the ground state of a Curie–Weiss ferromagnet and numerically on the search for ground-states in the three-dimensional  $\pm J$  spin-glass and in the SK model — both problems believed to be NP-hard.

We estimate the time-complexity of the algorithm to be  $\mathcal{O}(tN(\log N)^2)$  for the  $\pm J$  model and  $\mathcal{O}(tN^2(\log N)^2)$  the SK model, for the linear move-class deflation schedule. We assume here correctness of the scaling  $d_0 = \mathcal{O}(\log N)$  for the initial size  $d_0$  of the move-class with system size  $N$ . In case of the exponential move-class deflation schedule, the  $(\log N)^2$  factors in the above estimates can be replaced by  $\log N$  factors.

We have seen that the exponential MCD schedule gives a significant reduction of the computational cost without degrading the results. Clearly, further improvements of these schedules are conceivable. Let us mention the possibility of reducing the move-class size probabilistically, e.g. to have distributions of the form  $\mathcal{P}_{\bar{d}}(d) \propto \exp(-d/\bar{d})$  for picking a move-size  $d$ , and gradually reducing  $\bar{d}$ . This always gives some scatter in the size of the move-class used at any time, which we have observed to be advantageous. Different forms for  $\mathcal{P}_{\bar{d}}(d)$  may be contemplated and might in some cases be expedient, which in particular exhibit *lower* cutoffs  $d_{\min}(\bar{d})$  — gradually reduced to 1 during move-class deflation — so as to prevent the occurrence of small moves at the beginning of an OMCD run.

Moreover, the basic heuristics of the algorithm expects large moves to be accepted in sufficiently wide valleys, and deeper down or in narrower energy valleys only smaller moves. This observation clearly lends itself to formulating strategies for an algorithmic self-control of the move-class reduction schedule depending on recent acceptance rates, which might eventually lead to further improvements of OMCDs efficiency.

One of the advantages of OMCD over simulated annealing is in the fact that it is not hampered by the freezing transitions in the same way as the single spin flip Metropolis algorithms are, when applied to problems for which the energy landscape is complex. Simulated annealing in its standard implementations is therefore inefficient when used significantly below freezing temperatures in problems with glassy dynamics. So, to obtain good low-lying energy configurations with such an algorithm, one is really ‘living on fluctuations’. The absence of freezing transitions in OMCD may well become one of its decisive assets when dealing with large scale problems.

As OMCD is driven by properties of complex phase spaces in ways different from simulated annealing or genetic algorithms, it may be used for phase space diagnostics as demonstrated in Sect. 5. We have seen that the SK model appears differently to MCD than the (presumably) simpler  $\pm J$  model and the ferromagnet. It should be noted however that we are only just beginning to learn how to decipher the kind of analysis presented there.

**Acknowledgement** We are indebted to A. Hartmann for helpful discussions, and for providing us with some ground-state configurations for the  $\pm J$  model which allowed us to perform further tests of the quality of our results.

## References

- [1] G.S. Grest, C.M. Soukoulis and K. Levin, Phys. Rev. Lett **56**, 1148 (1986); G.S. Grest, C.M. Soukoulis, K. Levin and R.E. Randelman, in: *Heidelberg Colloquium on Glassy Dynamics*, edited by, J.L. van Hemmen and I. Morgenstern, (Springer, Berlin, Heidelberg, 1987)
- [2] W. Krauth and M. Mézard, J. Physique **50**, 3057 (1989)
- [3] H. Horner, Z. Phys B**86**, 291 (1992)
- [4] H. Patel, Z. Phys B**91**, 257 (199?)
- [5] M.R. Garey and D.S. Johnson, *Computers and Intractability*, (Freeman, New York, 1979)
- [6] S. Kirkpatrick, C.D. Gelatt, Jr., and M.P. Vecchi, Science **220**, 671 (1983)
- [7] S. Kirkpatrick, J. Stat. Phys. **34**, 975 (1984)
- [8] N. Metropolis, A. Rosenbluth, M. Rosenbluth, A. Teller, and E. Teller, J. Chem. Phys. **21**, 1087 (1953)
- [9] G. Dueck and T. Scheuer, J. Comp. Phys. **90**, 161 (1990)
- [10] J.H. Holland, *Adaptation in Natural and Artificial Systems*, (University of Michigan Press, Ann Arbor, 1975)
- [11] R. Kühn and G. Pöppel, unpublished manuscript (1993); Yu-Cheng Lin, Diploma Thesis, Heidelberg (1998), unpublished
- [12] D. Sherrington and S. Kirkpatrick, Phys. Rev. Lett **35**, 1792 (1975)
- [13] S.F. Edwards and P.W. Anderson, J. Phys. F**5**, 965 (1975)
- [14] D. Vertechi and M.A. Virasoro, J. Physique **50**, 2325 (1989)
- [15] H. Kinzelbach, PhD thesis, Heidelberg (1990), unpublished
- [16] H. Kinzelbach and H. Horner, Z. Phys B**84**, 95 (1991)
- [17] W.H. Press, S.A. Teukolsky, W.T. Vetterling, and B.P. Flannery, *Numerical Recipes in C*, (Cambridge University Press, Cambridge, 1992)
- [18] B.A. Berg, U.E. Hansmann, and T. Celik, Phys. Rev. B**50**, 16444 (1994)
- [19] U. Gropengiesser, J. Stat. Phys. **79**, 1005 (1995)
- [20] K.F. Pál, Physica A**223**, 283 (1996)
- [21] A.K. Hartmann, Europhys. Lett. **40**, 429 (1997)
- [22] G. Parisi, J. Phys A**13**, L115 (1980)